World Journal of Pharmaceutical Science and Research

www.wjpsronline.com

Research Article

ISSN: 2583-6579
SJIF Impact Factor: 6.916
Year - 2026
Volume: 5; Issue: 5
Page: 695-709

# PHYTOCHEMICAL, ANTIOXIDANT, AND IN SILICO ANTIBACTERIAL STUDY OF *SYZYGIUM MALACCENSE* EXTRACT AGAINST FLUOROQUINOLONE RESISTANCE

**Wisdom D. Cleanclay*[1,2], Segunoke S. Temiloluwa[1], Olasinde A. Ololade[1], Ifunanya K. Metu[1], Temidayo O. Adigun[3], Tebamifor E. Mercy1[2]**

[1]Department of Biochemistry (Covenant University) Ota, Ogun State, Nigeria.

[2]Covenant Applied Informatics and Communication Africa Centre of Excellence, Covenant University, Ota, Nigeria.

[3]Department of Biochemistry (University of Ilorin) Ilorin, Kwara State, Nigeria.

***Article Received: 31 March 2026*** | | ***Article Revised: 21 April 2026*** | | ***Article Accepted: 11 May 2026***

***Corresponding Author: Wisdom D. Cleanclay**
Department of Biochemistry (Covenant University) Ota, Ogun State, Nigeria.
**DOI:** https://doi.org/10.5281/zenodo.20233550

**How to cite this Article:** Wisdom D. Cleanclay, Segunoke S. Temiloluwa, Olasinde A. Ololade, Ifunanya K. Metu, Temidayo O. Adigun, Tebamifor E. Mercy (2026) PHYTOCHEMICAL, ANTIOXIDANT, AND IN SILICO ANTIBACTERIAL STUDY OF *SYZYGIUM MALACCENSE* EXTRACT AGAINST FLUOROQUINOLONE RESISTANCE. World Journal of Pharmaceutical Science and Research, 5(5), 695-709.



**ABSTRACT**

Background: Antibiotic resistance amongst other antimicrobial resistance remains a growing threat to global health, with more than 23 million confirmed cases of bacterial infections reported between 2016 and 2023. Fluoroquinolone resistance by bacteria species causes community acquired or healthcare-associated urinary tract infections and intra-abdominal infections, with over 50% of infections in some parts of the world, particularly in Asia. This study assessed the phytochemical, in vitro antioxidant and in silico antibacterial properties of fresh (AAJ1) and fermented (AAJ2) aqueous extracts of Syzygium malaccense on selected biomarkers in fluoroquinolone resistance. Materials and Methods: Fruits of Syzygium malaccense were plucked from the orchards of Covenant University. The phytochemical constituents of AAJ1 and AAJ2 were assessed using phytochemical screening assays and gas chromatography-mass spectrometry (GC-MS). The antioxidant activity was investigated using 2,2-diphenyl-1-1-picrylhydrazyl radical (DPPH) and ferric reducing antioxidant power assays (FRAP). Molecular docking was carried out to compare binding affinities of standard inhibitors and phytochemical constituents of AAJ1 against selected biomarkers. Results and Conclusion: Qualitative phytochemical screening showed that Syzygium malaccense extract contains flavonoids, phenols, and anthocyanins. The total phenolic content for AAJ1 and AAJ2 was 0.750 ± 0.12 mgGAE/ml and 1.005 ± 0.31 mgGAE/ml respectively. The total flavonoids content for AAJ1 and AAJ2 was 1.037 ± 0.09 mgQE/ml and 1.092 ± 0.06 mgQE/ml respectively. GC-MS chromatogram revealed the presence of 12 compounds. The most abundant phytochemicals were 2-butoxy-ethanol (54%), Hexamethyl-cyclotrisiloxane (17%) and octamethyl-cyclotetrasiloxane (6%). Oleonitrile and 3-methyl-5-phenyl-1H-1,3,4-benzotriazepin-2(3H)-one exhibited higher binding affinity for DNA gyrase and topoisomerase IV than the standard inhibitors. In conclusion, certain phytochemicals present in Syzygium malaccense are likely to be potential therapeutic candidates for fluoroquinolone-resistant infections.

**KEYWORDS:** Fluoroquinolone resistance, Syzygium malaccense, Molecular docking, GC-MS, antioxidant assays. Microbes, Microbiome, Antimicrobial resistance, and the emerging One-health (Health).

## INTRODUCTION

According to the Global antibiotic resistance (AR) surveillance report 2025, AR remains a growing threat to global health, with more than 23 million confirmed cases of bacterial infections reported between 2016 and 2023. Fluoroquinolone resistance causes community acquired or healthcare- associated urinary tract infections and intra-abdominal infections, causing over 50% of infections in some parts of the world, particularly in Asia. Syzygium malaccense was extracted, concentrated in a rotary evaporator before phytochemical and in silico antibacterial screening was carried out on fresh (AAJ1) and fermented (AAJ2) aqueous fruit extract. AAJ 1 and AAJ2 contained phenols, flavonoids and anthocyanins which showed great antioxidant properties. Molecular docking was carried out to compare binding affinities of standard inhibitors and phytochemical constituents which were found through GC-MS screening. Oleo nitrile had higher binding affinity for Topoisomerase IV ParC subunit than the standard (3S)-10-[(3R)-3-(1-aminocyclopropyl)pyrrolidin-1-yl]-9-fluoro-3-methyl- 5-oxo-2,3-dihydro-5H-[1,4]oxazino[2,3,4-ij]quinoline-6-carboxylic acid.3-Methyl-5-phenyl-1H- 1,3,4-benzotriazepin-2(3H)-one exhibited higher binding affinity for DNA gyrase than the standard trovafloxacin. Ultimately, phytochemicals from the aqueous extract of Syzygium malaccense may be potential therapeutic candidates for fluoroquinolone-resistant infections.

## MATERIALS AND METHODS

### Extract preparation

298g of Syzygium malaccense was handpicked from the grounds in Canaan Land, Ota and was thoroughly cleaned, washed and blended with 2 litres of distilled water in a blender to obtain an extract. It was filtered with an eight-fold muslin cloth followed by filter paper filtration, and left to sit for 24 hours. It was concentrated using a rotary evaporator and stored to be used for subsequent analyses. The fermented aqueous extract is denoted as AAJ1. 150 g of Syzygium malaccense was washed and combined with 1 litre of water to obtain an extract which was filtered with a muslin cloth and stored at 10 degrees Celsius. It was further concentrated in a rotary evaporator and stored until needed for subsequent analyses. The fresh aqueous extract is denoted as AAJ 2.

### Phytochemical screening

All qualitative phytochemical screening for saponins, alkaloids, flavonoids, terpenoids, cardiac glycosides, glycosides, tannins, quinones, anthocyanin, coumarins, anthraquinones and steroids was carried out using the techniques of Roghini & Vijayalakshmi (2018). Subsequently, quantitative estimation of flavonoids and total phenolics content was carried out following standard protocols (Phuyal et al. (2020). The gas chromatography-mass spectrometry (GC-MS) analysis was conducted using an AOC-20i autosampler connected to a mass spectrometer. The setup included a capillary column measuring 0.25 millimetres in width and 30 meters in length. The column oven was set to 80 degrees Celsius, the injection chamber to 254 degrees Celsius, and the pressure chamber to 108.0 kPa. The total flow through the column was 6.20 mL/min, with a column flow of 1.58 mL/min. The linear velocity was set to 46.3 cm/sec, and the flow rate for purging was 3.0 mL/min. Peak area normalization was employed to evaluate the relative proportions of the crude extract components.

### Antioxidant assays

The antioxidant capacity of the samples was assessed using three antioxidant assays on AAJ1 and AAJ2: Total Antioxidant Capacity (TAC) assay, Ferric Reducing Antioxidant Power (FRAP) assay and DPPH (2,2-diphenyl-1-picryl-hydrazyl-hydrate) free radical method (Babando et al., 2014).

**Molecular docking analysis**

Glide standard precision docking and molecular mechanics-generalized born surface area area calculations.

The fresh aqueous juice extract of Syzigium malaccense (AAJ2) and its constituent phytochemicals separated by the GC-MS techniques was used for the molecular docking analysis. A sampled flexible ligand (based on nitrogen inversion and ring conformations) was docked into the target receptor grid using glide standard precision docking, and post-docking minimization was carried out. Input partial charges were used to calculate the docking score, and ligands with more than 500 atoms were not docked or scored. The docking score was increased by the Epik state penalties and the van der Waals radii of ligand atoms with partial atomic charge were scaled back by 0.80 compared to the partial charge cut-off of 0.15.

Using the VSGB solvation model and the input ligand partial charges, Prime was also used to determine the molecular mechanics generalized Born surface area free energy change (MMGBSA ΔG) of the docked ligands. All processed ligands were used in the energy calculations, the flexible residues were constrained, and the Glide extra precision (XP) feature was used to perform more accurate and flexible docking on the defined receptor grid.

**Glide quantum polarized ligand docking**

Using the standard semi-empirical method precision, the initial Glide docking ligand charges were created. The pose was discarded as duplicate if the root mean square deviation was less than 0.5 angström and the maximum atomic displacement was less than 1.3. The Coulson charge semi-empirical method was used to determine the quantum mechanics charges for free ligands in the gas phase prior to redocking at standard precision. The Glide Score was used to determine which ligands had the best binding positions, while the van der Waals scaling for the receptor and ligand was 1.0 and 0.8, respectively.

**Protein-ligand interaction analysis**

The Glide merging procedure was used to create the docked ligands in complex with the targets and their corresponding binding poses. The Schrodinger PyMol® was used to represent the active pocket view of interactions while the Glide ligand interaction 2D visualizer was also employed for post-quantum polarized ligand docking protein-ligand visualization.

**Table 1: Study Targets and Corresponding PDB IDs and Standard Inhibitors.**

| Study Target | Description | PDB ID | Standard Inhibitor |
|---|---|---|---|
| DNA Gyrase | Quinolone (Trovafloxacin)- DNA cleavage complex of DNA gyrase from S. pneumoniae | 4Z2E | Trovafloxacin |
| Topoisomerase IV ParC | Klebsiella pneumoniae Topoisomerase IV (ParE-ParC) in complex with DNA and (3S)-10-[(3R)-3-(1-aminocyclopropyl)pyrrolidin-1-yl]-9-fluoro-3-methyl-5-oxo-2,3-dihydro-5H-[1,4]oxazino[2,3,4-ij]quinoline-6-carboxylic acid (compound 25) | 7LHZ | (3S)-10-[(3R)-3-(1-aminocyclopropyl) pyrrolidin-1-yl]-9-fluoro-3-methyl-5-oxo-2,3-dihydro-5H-[1,4]oxazino[2,3,4-ij]quinoline-6-carboxylic acid |

**RESULTS**

**Qualitative phytochemical analysis**

The table below shows the results for the qualitative phytochemical analysis of AAJ1 and AAJ2. The samples contain flavonoids, phenols, terpenoids, cardiac glycosides and anthocyanins.

**Table 1: Results for qualitative phytochemical analysis.**

| PHYTOCHEMICALS | AAJ1 | AAJ2 |
|---|---|---|
| Tannins | - | - |
| Saponins | - | - |
| Alkaloids | - | - |
| Flavonoids | + | + |
| Glycosides | - | - |
| Quinones | - | - |
| Phenol | + | + |
| Terpenoids | - | - |
| Cardiac glycosides | + | + |
| Steroids | - | - |
| Anthocyanin | + | + |
| Betacyanin | - | - |
| Coumarin | - | - |

+: detected; -: not detected.

**Quantitative phytochemical analysis**

**Table 2: Total flavonoids and phenols in Syzigium malaccense.**

| Sample | Standard | AAJ1 | AAJ2 |
|---|---|---|---|
| Total phenols (mg GAE/ml) | 5.01 ± 0.29 | 0.750±0.12 | 1.005±0.31 |
| Total flavonoids (mg QE/ml) | 1.196± 0.04 | 1.037±0.09 | 1.092± 0.06 |

Standard for total phenols: Gallic acid; Standard for total flavonoids: Quercetin; Standard for tannins: Gallic acid; GAE: Gallic acid equivalent; QE: Quercetin equivalent Values represent mean ± standard deviation, (n=3);

**In vitro antioxidant activity**

**DPPH ANTIOXIDANT ACTIVITY**

**Table 3: Inhibitory Concentration (IC50) values for fermented and fresh aqueous juice extract of Syzigium malaccense.**

| | AAJ1 | AAJ2 |
|---|---|---|
| IC50 | 0.492 ± 0.23 | 0.755 ± 0.36 |

Values represent mean ± standard deviation, (n=3); AAJ1; AAJ2: fermented and fresh aqueous juice extract of Syzigium malaccense respectively

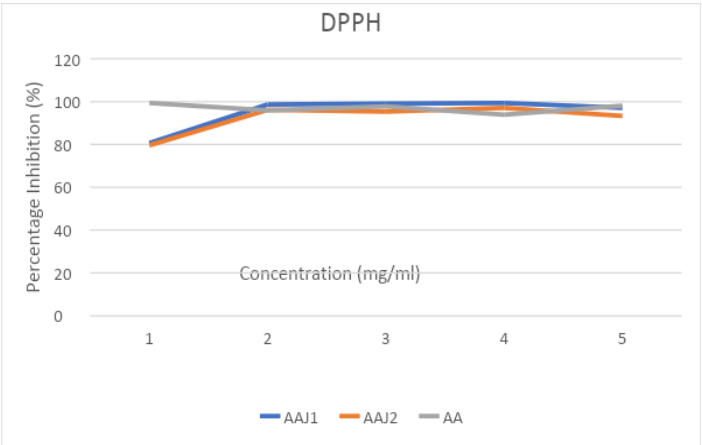


**Figure 1: Diphenyl–1 picrylhydrazyl antioxidant assay of fermented and fresh aqueous juice extract of Syzigium malaccense.**

**Ferric reducing antioxidant power assay**

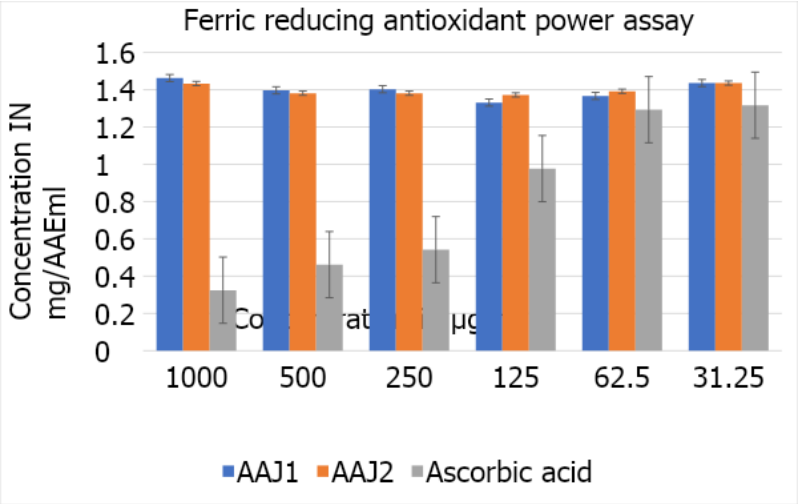


**Figure 2: Ferric reducing antioxidant power assay of fermented and fresh aqueous juice extract of Syzigium malaccense.**

## GAS CHROMATOGRAPHY-MASS SPECTROSCOPY PROFILING

Gas chromatography-mass spectroscopy profiling chromatograms for AAJ1, AAJ2 and AAJ3 are shown below. The presence of identified compounds was confirmed using the molecular weight, retention time and the peak area. The chromatogram identified 12 compounds for AAJ1 and 13 compounds for AAJ2.

The chromatogram revealed the presence of 12 compounds. The most abundant phytochemicals were 2-butoxy-ethanol (54%), Hexamethyl-cyclotrisiloxane (17%) and octamethyl-cyclotetrasiloxane (6%). The least abundant were tetradecane (1.27%) and hexadecane (1.32%).

**Table 4: Phytochemical compounds identified for various peaks in AAJ1.**

| Peak number | RT (min) | Area (%) | Height | Peak Width 50% (min) | Name |
|---|---|---|---|---|---|
| 1 | 3.31 | 9715910 | 1740858 | 0.383 | Cyclotrisiloxane, hexamethyl- |
| 2 | 4.432 | 30278011 | 8583971 | 0.526 | Ethanol, 2-butoxy- |
| 3 | 5.696 | 3501587 | 1295033 | 0.269 | Cyclotetrasiloxane, octamethyl- |
| 4 | 6.228 | 656576 | 462380 | 0.109 | 3H-1,3,4-Benzotriazepin-2-one, 1,2-dihydro-3-methyl-5-phenyl- |
| 5 | 7.075 | 3482426 | 1933528 | 0.126 | 2-Butoxyethyl acetate |
| 6 | 8.019 | 942229 | 585135 | 0.143 | Cyclopentasiloxane, decamethyl- |
| 7 | 10.422 | 872912 | 536620 | 0.166 | Cyclohexasiloxane, dodecamethyl- |
| 8 | 11.338 | 817788 | 509433 | 0.172 | Tetradecane |
| 9 | 12.603 | 698167 | 363067 | 0.149 | Cycloheptasiloxane, tetradecamethyl- |
| 10 | 13.764 | 740890 | 450510 | 0.143 | Hexadecane |
| 11 | 17.008 | 1371414 | 408599 | 0.24 | Hexadecanenitrile |
| 12 | 18.777 | 2364119 | 403183 | 0.246 | Oleanitrile |

**Table 5: Phytochemical Compounds Identified for Various Peak in AAJ2.**

| Peak number | RT (min) | Area (%) | Height | Peak Width 50% (min) | Name |
|---|---|---|---|---|---|
| 1 | 3.31 | 8478584 | 1454232 | 0.36 | Cyclotrisiloxane, hexamethyl- |
| 2 | 4.432 | 31324839 | 8668074 | 0.607 | Ethanol, 2-butoxy- |
| 3 | 5.696 | 2855027 | 1123398 | 0.177 | Cyclotetrasiloxane, octamethyl- |
| 4 | 7.075 | 2817307 | 1552064 | 0.114 | 2-Butoxyethyl acetate |
| 5 | 8.019 | 858828 | 512895 | 0.137 | Cyclopentasiloxane, decamethyl- |

| | | | | | |
|---|---|---|---|---|---|
| 6 | 10.417 | 837510 | 505070 | 0.183 | Cyclohexasiloxane, dodecamethyl- |
| 7 | 11.338 | 713896 | 470758 | 0.086 | Tetradecane |
| 8 | 12.603 | 716046 | 367150 | 0.177 | Cycloheptasiloxane, tetradecamethyl- |
| 9 | 13.764 | 745577 | 460821 | 0.149 | Hexadecane |
| 10 | 17.003 | 1932157 | 603874 | 0.252 | Pentadecanenitrile |
| 11 | 18.777 | 3978193 | 638351 | 0.246 | Oleanitrile |
| 12 | 18.954 | 874667 | 243267 | 0.229 | 1-Cyclohexen-2-ol, 3-(3-oxopropyl)- |

**Table 6: Phytochemical Compounds Identified for Various Peak in AAJ3.**

| Peak number | RT (min) | Area (%) | Height | Peak Width 50% (min) | Name |
|---|---|---|---|---|---|
| 1 | 3.236 | 1634707 | 377089 | 0.217 | beta.-D-Ribopyranoside, methyl |
| 2 | 4.048 | 46130 | 121062 | 0.057 | D-(-)-threo-2-Amino-1-(p-nitrophenyl)-1,3-propanediol |
| 3 | 4.157 | 133248 | 161433 | 0.092 | Urea, N-methyl-N-nitroso- |
| 4 | 5.69 | 374536 | 193320 | 0.16 | Cyclotetrasiloxane, octamethyl- |
| 5 | 8.019 | 71819 | 117545 | 0.074 | Hexanoic acid, 6-bromo- |
| 6 | 10.423 | 20124 | 80972 | 0.052 | Butanoic acid, 3-methyl- |
| 7 | 21.592 | 21947 | 79001 | 0.069 | Cyclotrisiloxane, hexamethyl- |

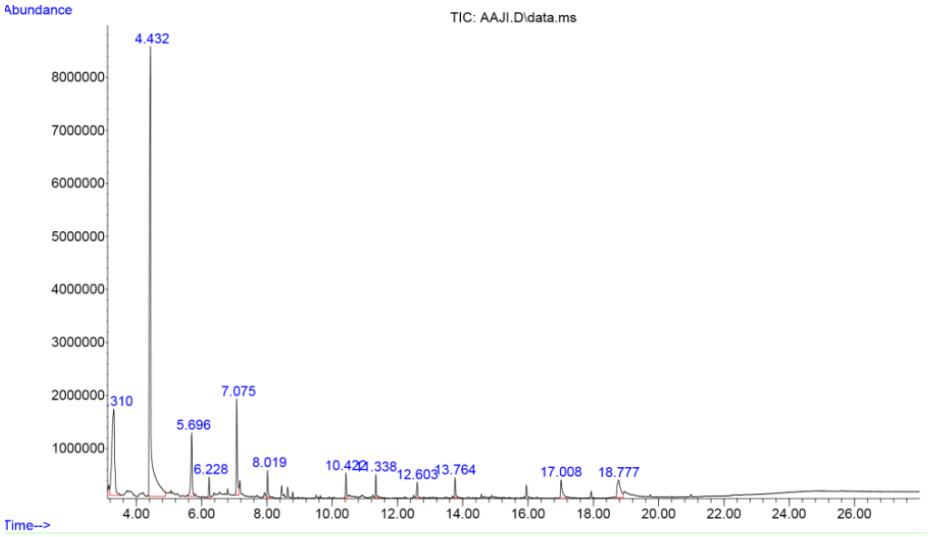


**Figure 3: GC-MS spectral chromatogram of AAJ1.**

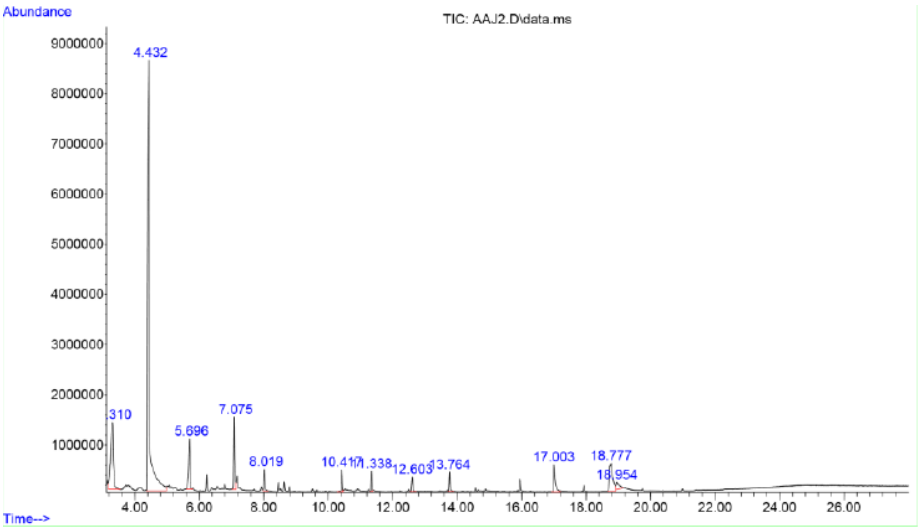


**Figure 4: GC-MS spectral chromatogram of AAJ2.**

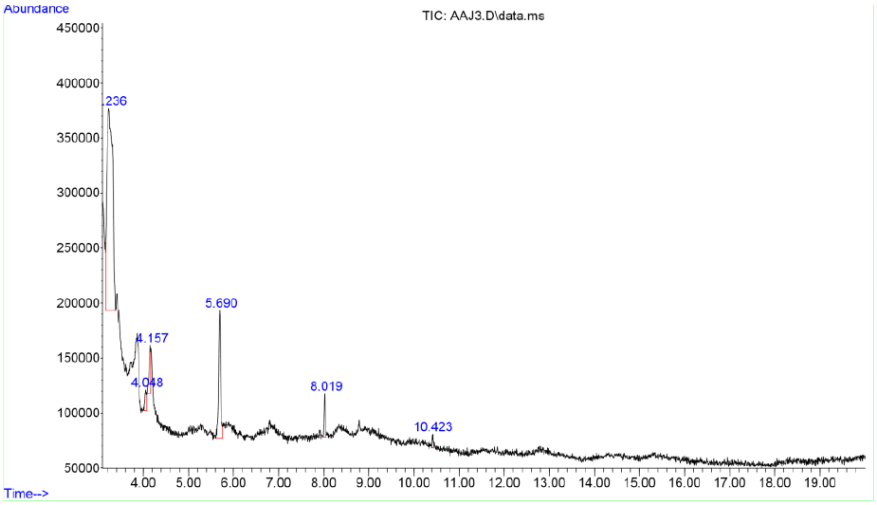


**Figure 5: GC-MS spectral chromatogram of AAJ3.**

**Molecular docking**

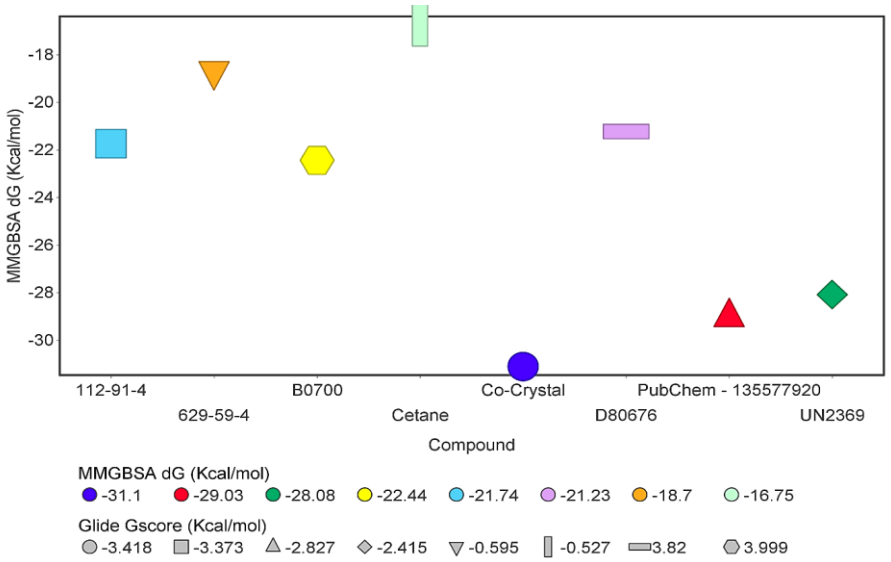


**Figure 6: Glide Standard Precision Docking Results of Quinolone-resistant Streptococcus pneumoniae DNA Gyrase.**

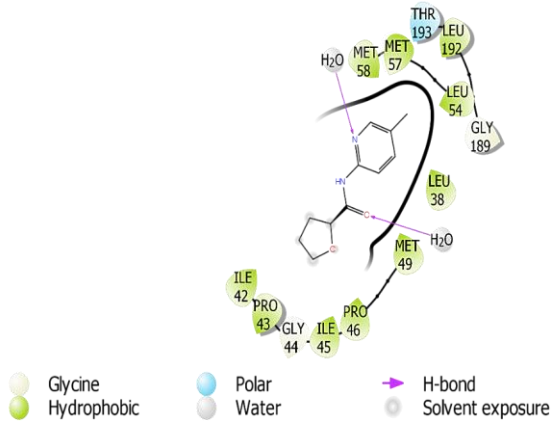


**Figure 7: Two-dimensional (2D) View of Interactions between SARS-CoV-2 NSP14 Co-Crystallized Ligand and NSP14 Following Quantum Polarized Ligand Docking.**

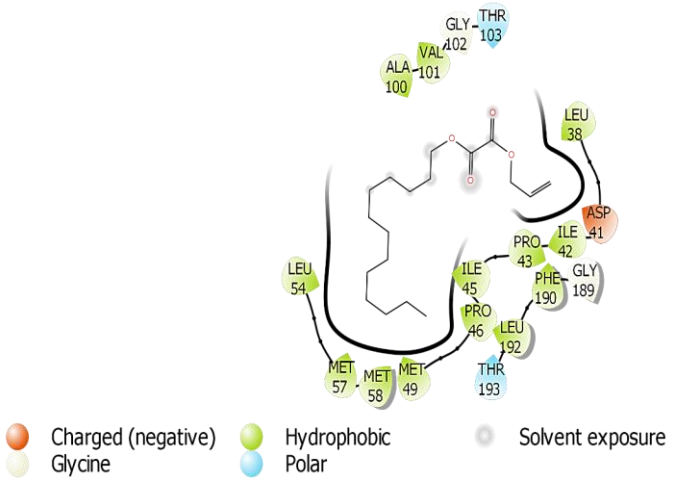


**Figure 8: Two-dimensional (2D) View of Interactions Between PubChem - 6420234 and SARS-CoV-2 NSP14 Following Quantum Polarized Ligand Docking.**

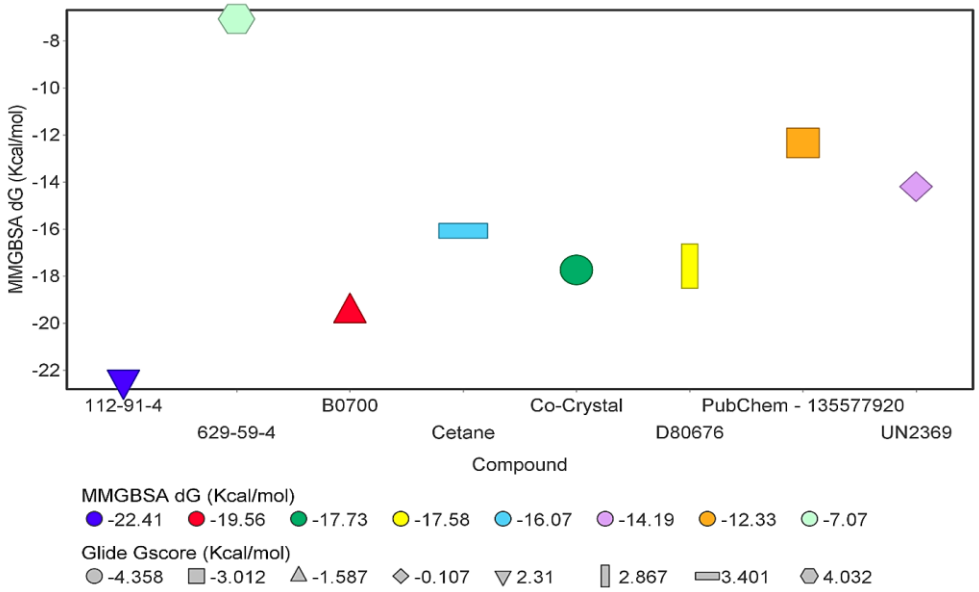


**Figure 9: Glide Standard Precision Docking Results of Klebsiella pneumoniae 342 Topoisomerase IV ParC.**

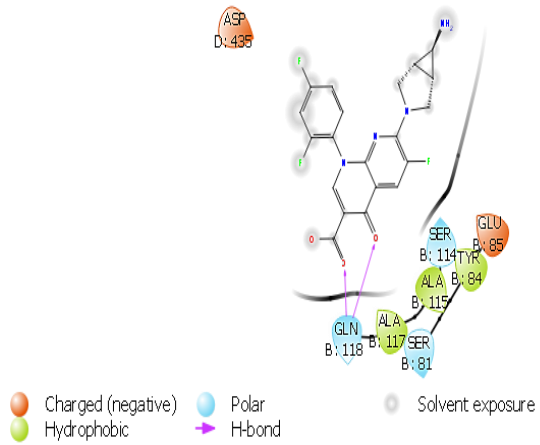


**Figure 10: Two-dimensional (2D) View of Interactions Between Human Furin Co-Crystallized Ligand and Human Furin Following Quantum Polarized Ligand Docking.**

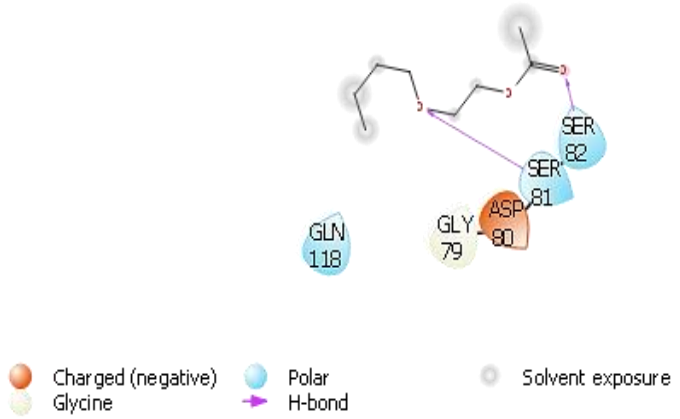


**Figure 11: Two-dimensional (2D) View of Interactions Between 119-62-0 and Human Furin Following Quantum Polarized Ligand Docking.**

**SARS-CoV-2 3CLpro**

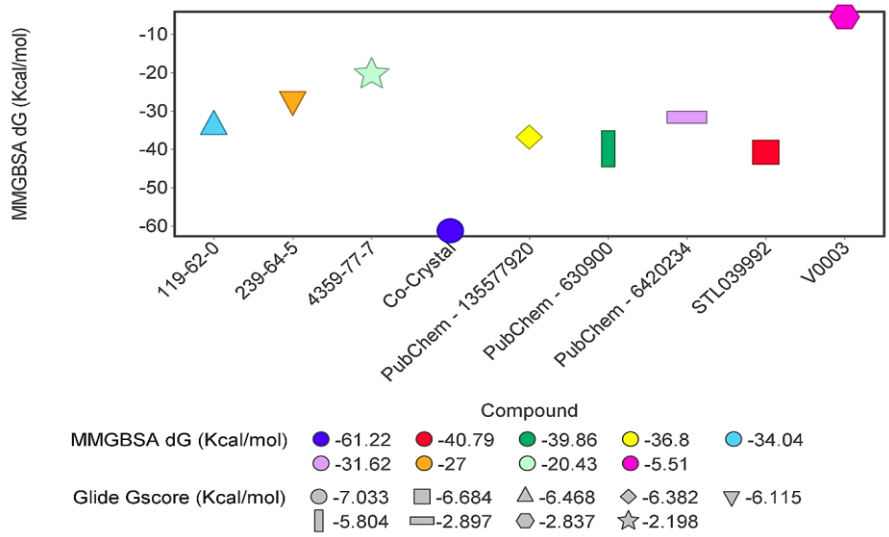


**Figure 12: Figure showing the binding affinity of hit compounds with SARS-CoV-2 3CLpro.**

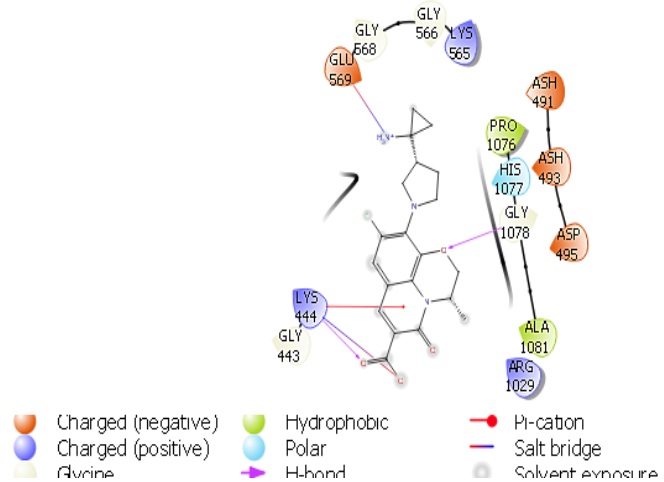


**Figure 13: Two-dimensional (2D) view of interactions between 3CLpro Co-Crystallized Ligand and 3CLpro following quantum polarized ligand docking.**

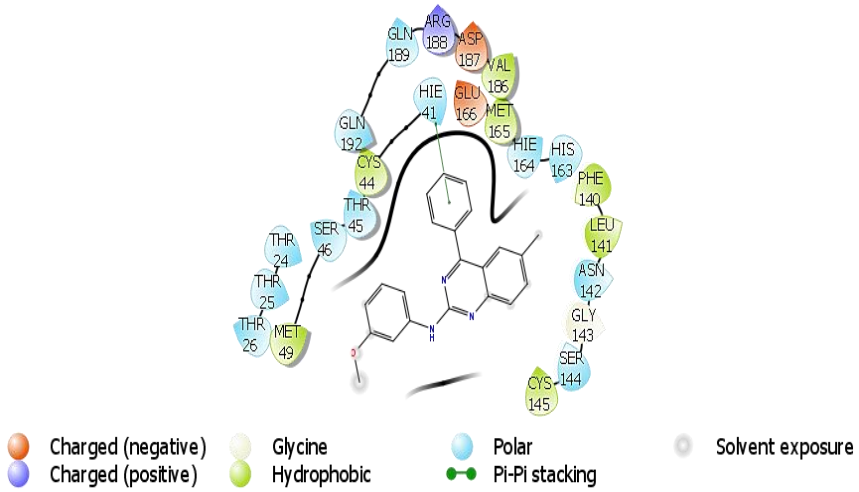


**Figure 14: Two-dimensional (2D) view of interactions between STL039992 and 3CLpro following quantum polarized ligand docking.**

**SARS-CoV-2 RNA-dependent RNA polymerase (RdRp)**

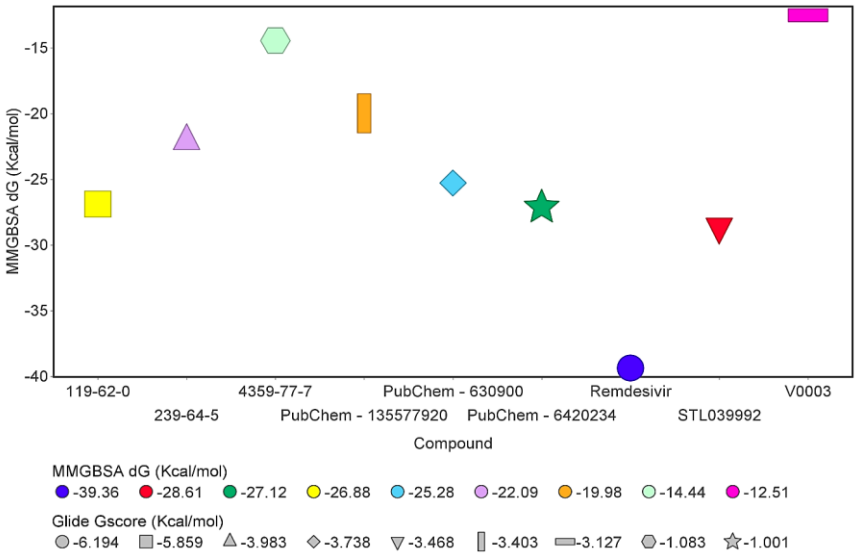


**Figure 15: Figure showing the binding affinity of hit compounds with SARS-CoV-2 RdRp.**

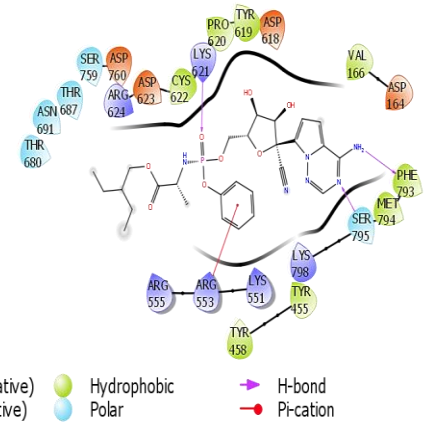


**Figure 16: Two-dimensional (2D) view of interactions between Remdesivir and SARS-CoV-2 RNA-dependent RNA Polymerase following quantum polarized ligand docking.**

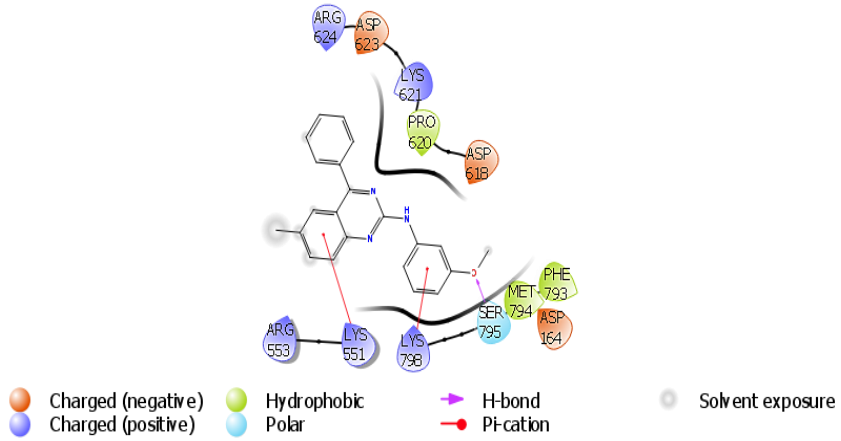


**Figure 17: Two-dimensional (2D) view of interactions between STL039992 and SARS-CoV-2 RNA-dependent RNA Polymerase following quantum polarized ligand docking.**

**SARS-CoV-2 Spike Protein**

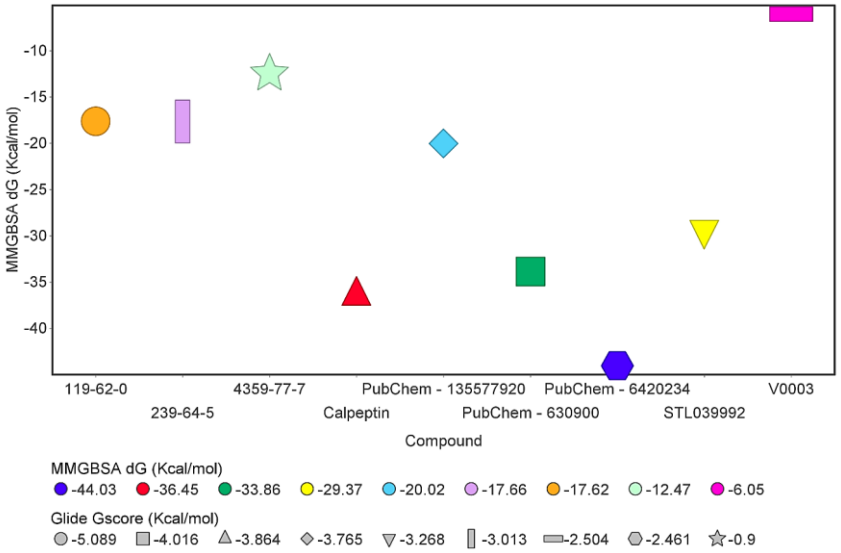


**Figure 18: Glide Standard Precision Docking Results of Klebsiella pneumoniae 342 Topoisomerase IV ParC.**

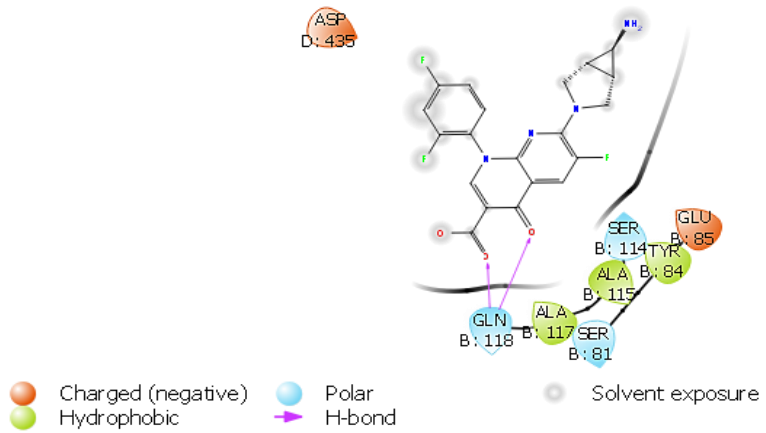


**Figure 19: Two-dimensional (2D) View of Interactions Between Streptococcus pneumoniae DNA Gyrase Co-Crystallized Ligand and Quinolone-resistant Streptococcus pneumoniae DNA Gyrase Following Quantum Polarized Ligand Docking**

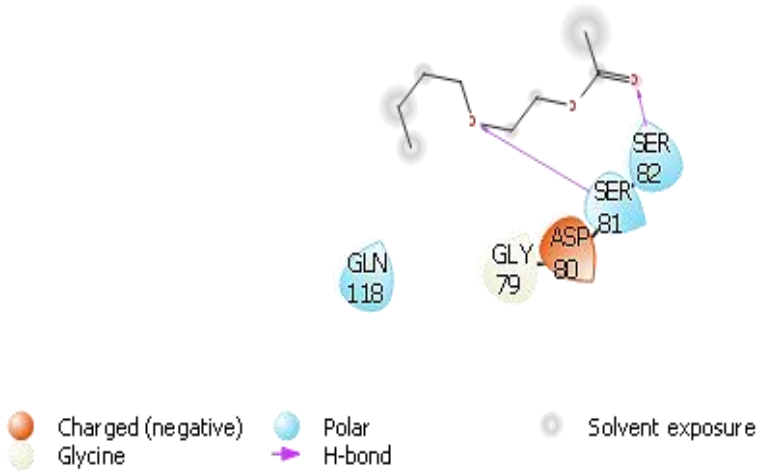


**Figure 20: Two-dimensional (2D) View of Interactions Between B0700 and Quinolone-resistant Streptococcus pneumoniae DNA Gyrase Following Quantum Polarized Ligand Docking.**

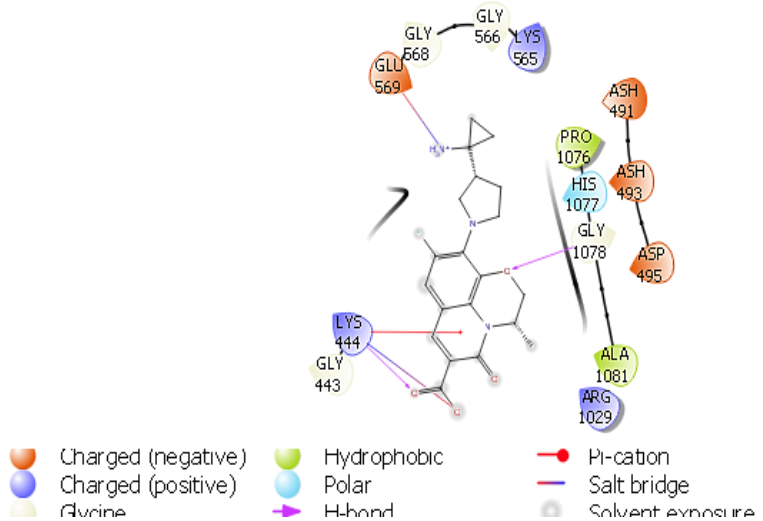


**Figure 4.8: Two-dimensional (2D) View of Interactions Between Klebsiella pneumoniae 342 Topoisomerase IV ParC Co-Crystal and Klebsiella pneumoniae 342 Topoisomerase IV ParC Following Quantum Polarized Ligand Docking.**

## DISCUSSION

Qualitative phytochemical studies of Syzygium malaccense extracts indicated the presence of flavonoids, phenols, and anthocyanins. Flavonoids and phenols have been proven to have antibacterial, antioxidant and anti-inflammatory properties. The presence of these phytochemicals in Syzygium malaccense may contribute to its ability as an antibacterial agent which corroborates the findings of (Ullah et al., 2022). The major phytochemicals identified were 3H-1,3,4-Benzotriazepin- 2-one, oleonitrile, 2-butoxy-ethanol, hexadecane (N-cetane) and tetradecane as reported in (Quenon et al., 2022). The molecular docking results shows that oleo nitrile had higher binding affinity for Topoisomerase IV ParC subunit than the standard (3S)-10-[(3R)-3-(1-aminocyclopropyl)pyrrolidin-1-yl]-9-fluoro-3-methyl-5-oxo-2,3-dihydro-5H-[1,4]oxazino[2,3,4-ij]quinoline-6-carboxylic acid.3-Methyl-5-phenyl- 1H-1,3,4-benzotriazepin-2(3H)-one exhibited higher binding affinity for DNA gyrase than the standard trovafloxacin. Cetane also showed high binding affinity for topoisomerase IV. The binding of cetane, hexadecane and 3H-1,3,4-Benzotriazepin-2-one tallies with the antibacterial studies carried out by (Deepak et al.,2019; Faridha Begum et al.,

2016; Glomb & Świątek, 2021). Hence, compounds identified from aqueous extract of S. malaccense show potential efficacy against fluoroquinolone resistant infections.

## CONCLUSION

From this study, Syzygium malaccense was shown to contain flavonoids and phenolics which have antibacterial and antioxidant properties. Syzygium malaccense also showed a high radical scavenging activity DPPH Free radical scavenging activity and ferric reducing antioxidant power assay (FRAP). From the molecular docking, 3-Methyl-5-phenyl-1H-1,3,4-benzotriazepin-2(3H)-one and oleonitrile present in Syzygium malaccense may be potential therapeutic candidates for fluoroquinolone- resistant infections.

## ACKNOWLEDGEMENTS

We duly acknowledge Covenant University for providing funds for the presentation of this research output at the Nigerian Society of Microbiology Conference (NSM 2023).

## REFERENCES

1. Adebayo, S.A., Dzoyem, J.P., Shai, L.J. & Eloff, J.N.,The anti-inflammatory and antioxidant activity of 25 plant species used traditionally to treat pain in southern African. BMC Complementary and Alternative Medicine, 2015; 15(1). doi:10.1186/s12906-015-0669-5.
2. Aldred, K.J., Kerns, R.J. & Osheroff, N., Mechanism of quinolone action and resistance. Biochemistry, 2014; 53 (10): 1565–1574. doi:10.1021/bi5000564.
3. Babando, A., Auwal, I., Muhammad, M. & Musa, A., Free radical scavenging and total antioxidant capacity of extracts of Anchomanes difformis Engl. (ARACEAE). Acta Poloniae Pharmaceutica, 2014; 70(1): 115–121. https://www.researchgate.net/publication/236274968.
4. Batista, Â.G., da Silva, J.K., Betim Cazarin, C.B., Biasoto, A.C.T., Sawaya, A.C.H.F., Prado, M.A. & Maróstica Júnior, M.R., Red-jambo (Syzygium malaccense): Bioactive compounds in fruits and leaves. LWT, 2017; 76: 284–291. doi:10.1016/j.lwt.2016.05.013.
5. Bisacchi, G.S., Origins of the Quinolone Class of Antibacterials: An Expanded 'Discovery Story'. Journal of Medicinal Chemistry, 2015; 58(12): 4874–4882. doi:10.1021/jm501881c.
6. Das, A.K., Islam, M.N., Faruk, M.O., Ashaduzzaman, M. & Dungani, R., Review on tannins: Extraction processes, applications and possibilities. South African Journal of Botany, 2020; 135: 58–70. doi:10.1016/j.sajb.2020.08.008.
7. David C. Hooper, Emerging mechanisms of fluoroquinolone resistance. Emerging Infectious Diseases, 2001; 7(2): 337–341. doi:https://doi.org/10.3201%2Feid0702.010239.
8. Dias, M.C., Pinto, D.C.G.A. & Silva, A.M.S., Plant flavonoids: Chemical characteristics and biological activity. Molecules, 2021; 26(17). doi:10.3390/molecules26175377.
9. Drlica, K., Malik, M., Kerns, R.J. & Zhao, X., Quinolone-mediated bacterial death. Antimicrobial Agents and Chemotherapy, 2008; 52(2): 385–392. doi:10.1128/AAC.01617-06.
10. Drlica K., Mechanism of fluoroquinlone action. Current Opinions in microbiology, 1999; 2: 504– 508.
11. Emmerson, A.M. & Jones, A.M., The quinolones: Decades of development and use. Journal of Antimicrobial Chemotherapy, 2003; 51(SUPPL. 1): 13–20. doi:10.1093/jac/dkg208.
12. Fàbrega, A., Madurga, S., Giralt, E. & Vila, J., Mechanism of action of and resistance to quinolones. Microbial Biotechnology, 2009; 2(1): 40–61. doi:10.1111/j.1751-7915.2008.00063.x.

13. Faridha Begum, I., Mohankumar, R., Jeevan, M. & Ramani, K., GC–MS Analysis of Bio- active Molecules Derived from Paracoccus pantotrophus FMR19 and the Antimicrobial Activity Against Bacterial Pathogens and MDROs. Indian Journal of Microbiology, 2016; 56(4): 426–432. doi:10.1007/s12088-016-0609-1.
14. Fernandes, F.A.N. & Rodrigues, S., Jambo—Syzygium malaccense. In: Exotic Fruits Reference Guide. Elsevier, 2018; pp. 245–249. doi:10.1016/B978-0-12-803138-4.00031-9.
15. Ghosh, D., Tannins from Foods to Combat Diseases. International Journal of Pharma Research & Review, 2015; 4(5): 40-45
16. Ginsburg, A.S., Hooper, N., Parrish, N., Dooley, K.E., Dorman, S.E., Booth, J., Diener-West, M., Merz, W.G., Bishai, W.R. & Sterling, T.R., Fluoroquinolone Resistance in Patients with Newly Diagnosed Tuberculosis. Clinical Infectious Diseases, 2003; 37(1): 1448–1452. doi:https://doi.org/10.1086/379328.
17. Glomb, T. & Świątek, P., Antimicrobial activity of 1,3,4-oxadiazole derivatives. International Journal of Molecular Sciences, 2021; 22(13). doi:10.3390/ijms22136979.
18. Goldstein, E.J.C., Goldstein, J.C. & Alden, R.M., Norfloxacin, a Fluoroquinolone Antibacterial Agent Classification, Mechanism of Action, and in Vitro Activity. The American journal of Medicine, 1978; 82(suppl 6B): 3–17. doi:10.3390/ijmm2215467.
19. Grossman, R.F., Hsueh, P.R., Gillespie, S.H. & Blasi, F., Community-acquired pneumonia and tuberculosis: differential diagnosis and the use of fluoroquinolones. International Journal of Infectious Diseases, 2014; 18(1): 14–21. doi:10.1016/J.IJID.2013.09.013.
20. Herbert, R., Caddick, M., Somerville, T., McLean, K., Herwitker, S., Neal, T., Czanner, G., Tuft, S. & Kaye, S.B., Potential new fluoroquinolone treatments for suspected bacterial keratitis. BMJ Open Ophthalmology, 2022; 7(1). doi:10.1136/bmjophth-2022-001002.
21. Hooper, D.C. & Jacoby, G.A., Mechanisms of drug resistance: Quinolone resistance. Annals of the New York Academy of Sciences, 2015; 1354(1): 12–31. doi:10.1111/nyas.12830.
22. Hooper, D.C. & Jacoby, G.A., Topoisomerase inhibitors: Fluoroquinolone mechanisms of action and resistance. Cold Spring Harbor Perspectives in Medicine, 2016; 6(9). doi:10.1101/cshperspect.a025320.
23. Hutchings, M., Truman, A. & Wilkinson, B., Antibiotics: past, present and future. Current Opinion in Microbiology, 2019; 51: 72–80. doi:10.1016/J.MIB.2019.10.008.
24. Imaga, N.A., Iheagwam, F.N. Asibe, C., Sogunle, T.B., & Chinedu, S.N., Antidiabetic modulatory effects of Vernonia amygdalina and Allium sativum combined extract in streptozotocin-induced diabetic rats, 2023; Vegetos 36(2): 615-625.
25. Iweala, E.J., AE Oluwapelumi, OE Dania, EA Ugbogu. Bioactive Phytoconstituents and Their Therapeutic Potentials in the Treatment of Haematological Cancers: A Review. Life, 2023; 13(7): 1422.
26. Iyanda-Joel, W.O., Olusayo B. Ajetunmobi, Shalom N. Chinedu, Emeka E. J. Iweala, Oluwatobi S. Adegbite, "Phytochemical, Antioxidant and Mitochondrial Permeability Transition Studies on Fruit-Skin Ethanol Extract of Annona muricata", Journal of Toxicology, 2019; Article ID 7607031. https://doi.org/10.1155/2019/7607031.
27. Jacoby, G.A., Strahilevitz, J. & Hooper, D.C., Plasmid-Mediated Quinolone Resistance. Microbiology Spectrum, 2014; 2(5). doi:10.1128/microbiolspec.PLAS-0006.
28. Karl, D., Xilin, Z. & Muhammad, M., Fluoroquinolone Resistance. Bacterial Resistance to Antibiotics - From molecules to Man, 2019; 1: 125. doi:https://doi.org/10.1002/9781119593522.ch6.

29. Khan, S., Khan, S.N., Akhtar, F., Misba, L., Meena, R. & Khan, A.U., Inhibition of multi-drug resistant Klebsiella pneumoniae: Nanoparticles induced photoinactivation in presence of efflux pump inhibitor. European Journal of Pharmaceutics and Biopharmaceutics, 2020; 157: 165–174. doi:10.1016/J.EJPB.2020.10.007.
30. Khare, T., Anand, U., Dey, A., Assaraf, Y.G., Chen, Z.S., Liu, Z. & Kumar, V., Exploring Phytochemicals for Combating Antibiotic Resistance in Microbial Pathogens. Frontiers in Pharmacology, 2021; 12. doi:10.3389/fphar.2021.720726.
31. Khoo, H.E., Azlan, A., Kong, K.W. & Ismail, A. (2016) Phytochemicals and Medicinal Properties of Indigenous Tropical Fruits with Potential for Commercial Development. Evidence-based Complementary and Alternative Medicine.2016. doi:10.1155/2016/7591951.
32. Lungu, I.A., Moldovan, O.L., Biriș, V. & Rusu, A., Fluoroquinolones Hybrid Molecules as Promising Antibacterial Agents in the Fight against Antibacterial Resistance. Pharmaceutics, 2022; 14(8). doi:10.3390/pharmaceutics14081749.